

Power and wavelength polarization bistability with very wide hysteresis cycles in a 1550nm-VCSEL subject to orthogonal optical injection

Antonio Hurtado,^{1,*} Ana Quirce,^{2,3} Angel Valle,² Luis Pesquera²
and Michael J. Adams¹

¹*School of Computer Science and Electronic Engineering, Wivenhoe Park, Colchester, CO4 3SQ, United Kingdom*

²*Instituto de Física de Cantabria, (CSIC-Univ. Cantabria), Avda. Los Castros s/n, E39005, Santander, Spain*

³*Dept. de Física Moderna, Fac. Ciencias, Univ. Cantabria, Avda. Los Castros s/n, E39005, Santander, Spain*
**ahurt@essex.ac.uk*

Abstract: We have measured optical power and wavelength polarization bistability in a 1550nm-Vertical Cavity Surface-Emitting Laser (VCSEL) subject to orthogonally-polarized optical injection into the orthogonal polarization of the fundamental transverse mode. Optical bistability with very wide hysteresis cycles, up to four times wider than previously reported results has been measured for both the optical power and wavelength domain. We also report the experimental observation of three different shapes of polarization bistability, anticlockwise, clockwise and X-Shape bistability, all of them with wide hysteresis cycles. This rich variety of behaviour at the important wavelength of 1550 nm offers promise for the use of VCSELs for all-optical signal processing and optical switching/routing applications.

©2009 Optical Society of America

OCIS codes: (140.7260) Vertical cavity surface emitting lasers; (190.1450) Bistability; (230.5440) Polarization-selective devices; (130.4815) Optical switching devices.

References and links

1. H. Kawaguchi, "Bistabilities and Nonlinearities in Laser Diodes," Norwood, MA: Artech House (1994).
2. F. Koyama, "Recent advances of VCSEL photonics," *J. Lightwave Technol.* **24**(12), 4502–4513 (2006).
3. Z. G. Pan, S. Jiang, M. Dagenais, R. A. Morgan, K. Kojima, M. T. Asom, R. E. Leibenguth, G. D. Guth, and M. W. Focht, "Optical injection induced polarization bistability in vertical-cavity surface-emitting lasers," *Appl. Phys. Lett.* **63**(22), 2999–3001 (1993).
4. Y. Hong, K. A. Shore, A. Larsson, M. Ghisoni, and J. Halonen, "Pure frequency-polarization bistability in vertical-cavity surface-emitting semiconductor lasers subject to optical injection," *Electron. Lett.* **36**(24), 2019–2020 (2000).
5. I. Gatara, J. Buesa, H. Thienpont, K. Panajotov, and M. Sciamanna, "Polarization switching bistability and dynamics in vertical-cavity surface-emitting laser under orthogonal optical injection," *Opt. Quantum Electron.* **38**(4-6), 429–443 (2006).
6. I. Gatara, K. Panajotov, and M. Sciamanna, "Frequency-induced polarization bistability in vertical-cavity surface emitting lasers with orthogonal optical injection," *Phys. Rev. A* **75**(2), 023804 (2007).
7. K. H. Jeong, K. H. Kim, S. H. Lee, M. H. Lee, B. S. Yoo, and K. A. Shore, "Optical injection-induced polarization switching dynamics in 1.5 μm wavelength single-mode vertical-cavity surface-emitting lasers," *IEEE Photon. Technol. Lett.* **20**(10), 779–781 (2008).
8. A. Hurtado, I. D. Henning, and M. J. Adams, "Two-wavelength switching with a 1550nm VCSEL under single orthogonal optical injection," *IEEE J. Sel. Top. Quantum Electron.* **14**(3), 911–917 (2008).
9. A. Valle, M. Gomez-Molina, and L. Pesquera, "Polarization bistability in 1550 nm wavelength single-mode vertical-cavity surface-emitting lasers subject to orthogonal optical injection," *IEEE J. Sel. Top. Quantum Electron.* **14**(3), 895–902 (2008).
10. A. Hurtado, I. D. Henning, and M. J. Adams, "Different forms of wavelength polarization switching and bistability in a 1.55 μm vertical-cavity surface-emitting laser under orthogonally polarized optical injection," *Opt. Lett.* **34**(3), 365–367 (2009).
11. A. Quirce, A. Valle, and L. Pesquera, "Very wide hysteresis cycles in 1550nm-VCSELs subject to orthogonal optical injection," *IEEE Photon. Technol. Lett.* **21**(17), 1193–1195 (2009).
12. A. Hurtado, I. D. Henning, and M. J. Adams, "Wavelength Polarization Switching and Bistability in a 1550nm-VCSEL subject to Polarized Optical Injection," *IEEE Photon. Technol. Lett.* **21**(15), 1084–1086 (2009).

13. C. F. Marki, S. Moro, D. R. Jorgesen, P. Wen, and S. C. Esener, "Cascadable optical inversion using 1550nm VCSEL," *Electron. Lett.* **44**(4), 292–293 (2008).
14. T. Katayama, T. Ooi, and H. Kawaguchi, "Optical buffer memory with shift register function using 1.55- μ m polarization bistable VCSELs," *The 21st Annual Meeting of the IEEE Lasers & Electro-Optics Society (LEOS 2008), ThG1*, pp. 739–740, Newport Beach, USA, November 13, 2008.
15. T. Katayama, T. Kitazawa, and H. Kawaguchi, "All-optical flip-flop operation using 1.55 μ m polarization bistable VCSELs," *Conference on Lasers and Electro-Optics/Quantum Electronics and Laser Science Conference (CLEO/QELS 2008), CME5*, San Jose, USA, May 5, 2008.
16. A. M. Kaplan, G. P. Agrawal, and D. N. Maywar, "All-optical flip-flop operation of VCSEA," *Electron. Lett.* **45**(2), 127–128 (2009).
17. W. L. Zhang, and S. F. Yu, "Optical Flip-Flop using Bistable Vertical-Cavity Semiconductor Optical Amplifiers with Anti-Resonant Reflecting Optical Waveguide," *J. Lightwave Technol.* **27**(21), 4703–4710 (2009).
18. K. Inoue, "All-optical flip-flop operation in an optical bistable device using two lights of different frequencies," *Opt. Lett.* **12**(11), 918–920 (1987).
19. D. N. Maywar, G. P. Agrawal, and Y. Nakano, "All-optical hysteresis control by means of cross-phase modulation in semiconductor optical amplifiers," *J. Opt. Soc. Am. B* **18**(7), 1003–1013 (2001).
20. M.-R. Park, O.-K. Kwon, W.-S. Han, K.-H. Lee, S.-J. Park, and B.-S. Yoo, "All-monolithic 1.55 μ m InAlGaAs/InP vertical cavity surface emitting lasers grown by metal organic chemical vapour deposition," *Jpn. J. Appl. Phys.* **45**(1), L8–L10 (2006).
21. A. Hurtado, I. D. Henning, and M. J. Adams, "Two-wavelength switching with 1.55 μ m VCSEA," *Electron. Lett.* **43**(16), 887–888 (2007).
22. P. Pakdeevanich, and M. J. Adams, "Switching powers for optical bistability in a semiconductor laser above and below threshold," *Opt. Commun.* **176**(1-3), 195–198 (2000).
23. A. Hurtado, A. Gonzalez-Marcos, J. A. Martin-Pereda, and M. J. Adams, "Two-wavelength switching with a distributed feedback semiconductor optical amplifier," *IEE Proc., Optoelectron.* **153**(1), 21–27 (2006).
24. P. Pakdeevanich, and M. J. Adams, "Measurements and modelling of reflective bistability in 1.55 μ m laser diode amplifiers," *IEEE J. Quantum Electron.* **35**(12), 1894–1903 (1999).
25. A. Hurtado, A. Gonzalez-Marcos, and J. A. Martin-Pereda, "Modeling reflective bistability in a vertical-cavity semiconductor optical amplifiers," *IEEE J. Quantum Electron.* **41**(3), 376–383 (2005).

1. Introduction

Bistable laser diodes and amplifiers are expected to be key components for use in optical telecommunication networks (for a review see [1]). In particular, Vertical-Cavity Surface Emitting Lasers (VCSELs) are very promising devices due to their inherent advantages in comparison to planar devices. These advantages include among others, reduced fabrication costs, high coupling efficiency to optical fibres, on-wafer testing capability, ease of fabrication of 2D arrays, single-mode operation, compactness, etc [2]. These features have attracted attention to the study of the nonlinear properties of VCSELs for potential use in optical signal processing, optical interconnects and optical switching applications.

Polarization switching (PS) and polarization bistability (PB) in VCSELs have undergone considerable research effort in the last years [3–14]. PS and PB have been reported experimentally [3–5] and theoretically [6] in short-wavelength VCSELs subject to orthogonal optical injection. More recently, attention has been focused on the analysis of PS and PB in long-wavelength VCSELs emitting in the region of 1550nm [7–14] (the most commonly used wavelength in present long-haul optical networks) and different practical applications, including logic gates [13], flip-flop operation [14] and a buffer memory [15] have been very recently reported. Different shapes of power and frequency PS and PB (anticlockwise and clockwise) have been observed in 1550nm-VCSELs subject to orthogonal optical injection [7–11] (as well as to different polarized optical injection [12]) into the orthogonal polarization of the fundamental mode of the device. However, in these works, either optical bistability was not observed [7] or the width of the hysteresis cycles associated to the occurrence of PB was either negligible or narrow [8–10] [12]. Only recently, experimental observation of frequency PB in a 1550nm-VCSEL with wide hysteresis cycles, up to 37 Ghz has been reported [11]. This fact could enhance the potential practical use of these devices in applications whose operation principle would be based in the width of the appearing hysteresis cycles associated to the bistability, such as all-optical bistable flip-flops or bistable memory elements, etc [16–19].

In this work, we have studied experimentally the Power and Wavelength Polarization Bistability in a 1550nm-VCSEL biased well above threshold and subject to orthogonally-polarised optical injection into the subsidiary orthogonal polarization mode of the device. The PB has been systematically studied for important system parameters, namely the applied bias

current and the initial wavelength detuning. The output powers of the emitting parallel polarization mode and the subsidiary orthogonal polarization mode of the 1550nm-VCSEL have been simultaneously studied and this technique has led to the experimental observation of different shapes of PB in a 1550nm-VCSEL, including anticlockwise, clockwise and X-Shape or butterfly bistability, all of them with wide hysteresis cycles, up to four times wider with respect to previously reported results [8]. This diversity of behaviour at 1550 nm, the most commonly used wavelength in optical telecommunication networks, offers promise for the use of VCSELs in optical signal processing and optical switching applications.

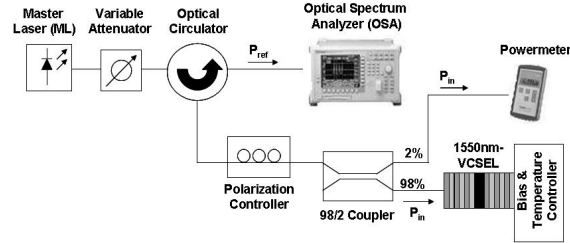


Fig. 1. Experimental setup used for the orthogonal optical injection in a 1550nm-VCSEL.

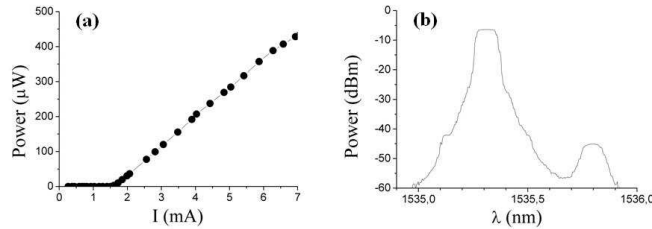


Fig. 2. (a) L-I curve and (b) spectrum of the 1550 nm-VCSEL.

2. Experimental setup

Orthogonally polarized optical injection is attained with the setup shown in Fig. 1. An all-fibre system has been used to inject the light from a tunable laser source (Master Laser, ML) into the 1550nm-VCSEL used in the experiments. A variable attenuator is included for the control of the optical power of the externally injected signal. The output of the ML is then injected into the VCSEL via a three-port optical circulator. The control of the polarization of the externally injected signal is performed by using a fibre polarization controller. A 98/2 fibre directional coupler divides the optical path in two branches; the 2% output of the coupler is connected to a power meter for the monitoring of the optical input power whereas the 98% coupler's output is directly connected to the 1550nm-VCSEL. Finally, an Optical Spectrum Analyzer (OSA) is connected to the third port of the optical circulator for the analysis of the reflective output of the VCSEL. Note that the power measured at the OSA includes the power emitted by the VCSEL plus the reflection of the input light.

The device used in the experiments was a commercially available quantum-well 1550nm-VCSEL (Raycan) [20]. Figure 2(a) plots the experimentally measured L-I curve of the VCSEL at the temperature of 298 K, showing a threshold current (I_{th}) of 1.64 mA. Figure 2(b) shows the measured spectrum of the VCSEL when biased with a current of 6.0 mA also at 298 K. The two modes appearing in Fig. 2(b) correspond to the two orthogonal polarizations of the fundamental transverse mode of the device. The lasing mode has parallel polarization and its wavelength, $\lambda_{||}$, is located at a wavelength of 1535.3 nm, while the subsidiary mode has orthogonal polarization and its wavelength, λ_{\perp} , is shifted 0.49 nm to the long-wavelength side of the lasing mode. Spectra of this form were measured for all biases and no polarization switching was observed for any applied bias current above the threshold value.

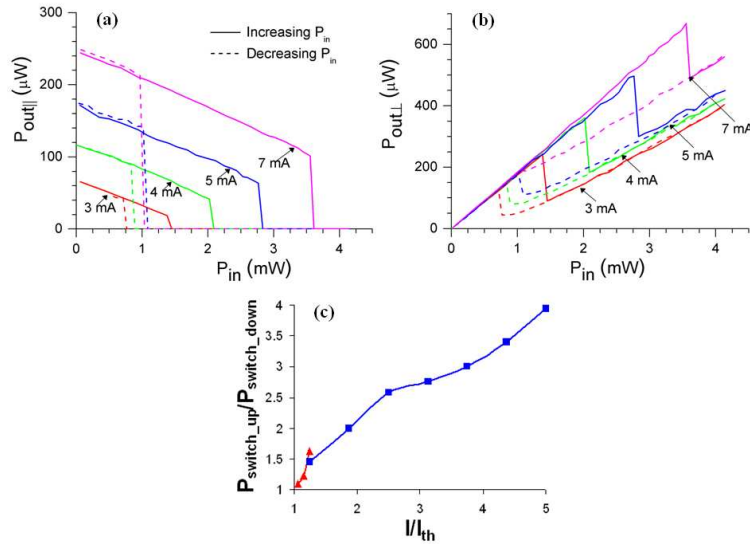


Fig. 3. I/O power characteristic for different levels of applied bias current and constant initial wavelength detuning of 0.15 nm for the (a) parallel and the (b) orthogonal polarization mode. (c) Width of the hysteresis cycle vs. applied bias current.

3. Experimental results and discussion

3.1 Optical power polarization bistability

Figures 3(a) and 3(b) show the input/output power characteristics for the parallel and the orthogonal polarization modes of the 1550nm-VCSEL for different levels of applied bias current to the device, namely 3 mA ($1.83 \times I_{th}$), 4 mA ($2.44 \times I_{th}$), 5 mA ($3.05 \times I_{th}$), and 7 mA ($4.27 \times I_{th}$). The initial wavelength detuning between the externally injected signal and the orthogonal polarization mode of the device was kept constant and equal in all cases to 0.15 nm. PB can be observed in the VCSEL under orthogonal optical injection when the optically injected power is high enough to lock the orthogonal polarization mode of the VCSEL to the wavelength of the externally injected signal. At that point PB is produced and the output of the parallel polarized mode of the VCSEL is suppressed whereas the output of the orthogonal polarized signal switches between two stable output states [3] [5] [8] [9]. As has been previously reported in short- [3] [5] and long-wavelength [8] [9] VCSELs, the results in Fig. 3(a) show that the output of the parallel polarized mode of the VCSEL exhibits clockwise optical bistability for all cases of applied bias current. At the same time, as can be seen in Fig. 3(b) the I/O characteristic of the orthogonal polarization mode of the VCSEL also shows clockwise bistability for all the biasing cases considered. The latter had only been recently reported in 1550nm-VCSEL [8] for cases of high enough initial wavelength detuning (in particular, 0.15nm in [8]). It is important to note here that prior to the onset of PB, the external optical injection produced slight shifts in the wavelength of the two polarization modes of the VCSEL and we believe that this may be due to frequency pulling effects. Figures 3(a) and 3(b) show that for both polarization modes of the device, as the applied bias current is increased well above threshold the more power is needed for the obtaining of optical bistability and also the width of the associated hysteresis cycles widen considerably. This behavior is the same as that observed for dispersive bistability in Vertical-Cavity Semiconductor Optical Amplifiers [21] and also in planar devices, including Fabry-Perot [22] and distributed feedback semiconductor laser amplifiers [23]. We believe therefore that the dispersive nonlinearity is also the physical phenomenon that explains the widening of the hysteresis cycles associated with the occurrence of PB as the bias current is increased well above threshold.

Figure 3(c) summarizes the measured widths of the hysteresis cycles for the VCSEL used here (blue squares) in comparison to previously reported results [8] (red triangles) showing the increase in the width of hysteresis as a result of biasing the device with levels of current well above threshold. In particular, the measured widths of the hysteresis cycles are up to four times larger than those reported previously. This result is of importance for the potential development of low-cost, low-power, high-speed all-optical bistable flip-flops as well as all-optical bistable memory elements with 1550nm-VCSELs for all-optical signal processing applications in optical communication networks. These functions can be easily obtained when large hysteresis widths are achieved for optical bistability, as has been reported in vertical-cavity [16] [17] as well as in edge-emitting devices [18] [19].

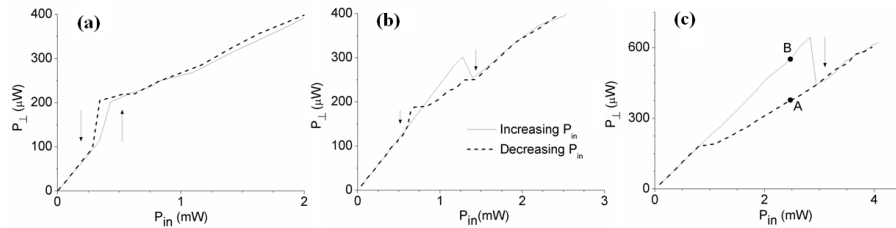


Fig. 4. I/O power characteristic for the output of the orthogonal polarization mode for three different levels of initial wavelength detuning of (a) 0.07nm, (b) 0.118nm and (c) 0.15nm and with constant bias current of 6mA ($3.66 \times I_{th}$).

Figures 3(a) and 3(b) also show that the simultaneous occurrence of clockwise bistability for both polarization modes of the VCSEL produces a drop in the total reflected output power (defined as the sum of the parallel and orthogonally polarized modes). This phenomenon is observed for high enough levels of initial wavelength detuning between the externally injected signal and the orthogonal polarized mode of the device [8]. The explanation for this drop in the total output power lies in the delicate balance between the different optical intensities in the device: the input, the reflected, the transmitted and the averaged intensity within the cavity [24] [25]. The higher the initial wavelength detuning, the more power needs to be injected in order to obtain switching between the two output states. This produces a higher drop in the gain associated with switching, which in turn favours the transmitted output of the device whereas the reflective output experiences a reduction of the on-off contrast ratio between output states. As a consequence, the shape of the nonlinear transition changes from anticlockwise bistability (for lower values of detuning) to the clockwise bistability appearing for higher values of detuning, as can be seen in Fig. 3(b).

The latter effect can be better seen in the influence of the initial wavelength detuning on the measured characteristics of the optical power PB. Figures 4 (a-c) show the input/output power relationships of the orthogonal polarization mode of the VCSEL for three different levels of initial wavelength detuning. Three different shapes of bistability, namely anticlockwise, X-Shape (or butterfly) and clockwise, appear as the initial wavelength detuning is increased, all of them with wide hysteresis cycles in comparison to previously reported results [8]. Therefore changes in the initial wavelength detuning modify the balance between the input, the transmitted, the reflected, and the averaged intensities leading to these three different types of bistable loops in the reflected transfer function of the VCSEL.

3.2 Wavelength polarization bistability

Wavelength polarization bistability is observed when the wavelength of the externally injected signal, λ_{ML} , is modified whilst the optical injected power is kept constant. Figures 5(a) and 5(b) show the output power of the parallel and the orthogonal polarization modes of the VCSEL as a function of the initial detuning between the wavelength of the externally injected signal (λ_{ML}) and the resonant wavelength of the orthogonal polarization mode of the device (λ_{\perp}). The results in Figs. 5(a) and 5(b) have been measured for increasing and decreasing λ_{ML} . Three different regions of bistability can be observed in Fig. 5(b) (marked from I to III)

similar to those obtained in [11]. In particular, the width of the hysteresis cycle of region III has been recently observed to be very large (up to 37 GHz wide) when high levels of input power or bias current are applied to the device [11]. Also, as seen in Fig. 5(b), region III is characterized by two stable states, A and B, which can be reached by increasing or decreasing λ_{ML} , respectively. Spectral measurements show that the A (B) state is characterized by the locking (unlocking) of the orthogonal polarization mode of the VCSEL to the wavelength of the externally injected signal, λ_{ML} . The upper (lower) limit of the III region corresponds therefore to the transition from locked to unlocked (unlocked to locked) output of the VCSEL when λ_{ML} is increased (decreased). These two stable states, A and B, are also marked in Fig. 4(c). The unlocked B state is reached by increasing P_{in} from small values. Further increase of P_{in} produces injection locking slightly below 3 mW. The locked A state can then be reached by decreasing P_{in} . The very large hysteresis width obtained for large wavelength detuning (see Fig. 4(c)) is a direct consequence of the large hysteresis width of region III.

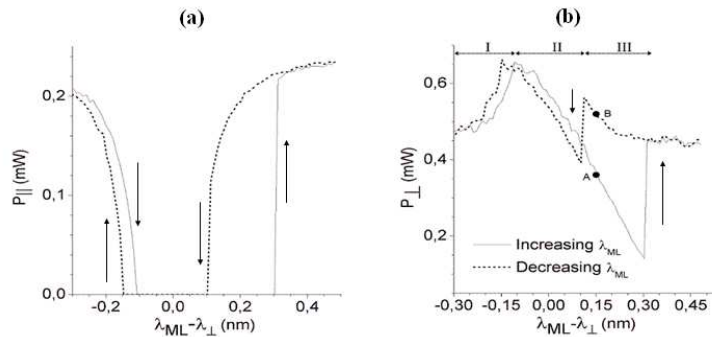


Fig. 5. Output power of (a) the parallel and (b) the orthogonal polarization mode of the VCSEL as a function of the initial wavelength detuning when increasing (solid lines) and decreasing (dashed lines) λ_{ML} , with $P_{in} = 2.5$ mW and applied bias current of 6 mA.

4. Conclusions

We have reported, for the first time to our knowledge, the experimental observation of optical power and wavelength polarization bistability with very wide hysteresis cycles in a 1550nm-VCSEL subject to orthogonal optical injection. The relationship between optical power and wavelength polarization bistabilities has been described. Three different shapes of polarization bistability, including anticlockwise, X-Shape and clockwise have been experimentally observed. In all cases, wide hysteresis cycles have been experimentally measured, up to four times higher than previously reported results. This diversity of behaviour in a VCSEL at the important telecom wavelength of 1550nm offers promise for the development of low-cost, low-power, high-speed all-optical bistable flip-flops, memory elements and logic gates for use in optical signal processing and optical switching applications in present and future optical telecommunication networks.

Acknowledgements

This work has been funded in part by the European Commission under the Programme FP7 Marie Curie Intra-European Fellowships Grant PIEF-GA-2008-219682 and by the Ministerio de Educación y Ciencia, Spain, Project TEC2006-13887-C) 5-02/TCM.